# Salinity has little effect on photosynthetic and respiratory responses to seasonal temperature changes in black mangrove (*Avicennia germinans*) seedlings

Michael J. Aspinwall[1*], Martina Faciane[2], Kylie Harris[1], Madison O'Toole[1], Amy Neece[1], Vrinda Jerome[1], Mateo Colón[1], Jeff Chieppa[1], and Ilka C. Feller[2]

[1]*Department of Biology, University of North Florida, 1 UNF Drive, Jacksonville, FL 32224 USA*

[2]*Department of Earth, Environmental and Planetary Sciences, Rice University, 6100 Main Street, Houston, TX 77005 USA*

[3]*Smithsonian Environmental Research Center, 647 Contees Wharf Road, Edgewater, MD 21037*

[*]Corresponding author email: m.aspinwall@unf.edu, phone: 1-904-620-5626

**Abstract**

Temperature and salinity are important regulators of mangrove range limits and productivity, but the physiological responses of mangroves to the interactive effects of temperature and salinity remain uncertain. We tested the hypothesis that salinity alters photosynthetic responses to seasonal changes in temperature and vapor pressure deficit (*D*), as well as thermal acclimation of leaf respiration in black mangrove (*Avicennia germinans*). To test this hypothesis, we grew seedlings of *A. germinans* in an outdoor experiment for ~12 months under four treatments spanning 0 to 55 ppt porewater salinity. We repeatedly measured seedling growth and *in situ* rates of leaf net photosynthesis ($A_{sat}$) and stomatal conductance to water vapor ($g_s$) at prevailing leaf temperatures, along with estimated rates of Rubisco carboxylation ($V_{cmax}$) and electron transport for RuBP regeneration ($J_{max}$), and measured rates of leaf respiration at 25 °C ($R_{area}^{25}$). We developed empirical models describing the seasonal response of leaf-gas exchange and photosynthetic capacity to leaf temperature and *D*, and the response of $R_{area}^{25}$ to changes in mean

daily air temperature. We tested the effect of salinity on model parameters. Over time, salinity had weak or inconsistent effects on $A_{sat,}$ $g_s$, and $R_{area}^{25}$. Salinity also had little effect on the biochemical parameters of photosynthesis ($V_{cmax}$, $J_{max}$) and individual measurements of $A_{sat}$, $g_s$, $V_{cmax}$, and $J_{max}$ showed a similar response to seasonal changes in temperature and *D* across all salinity treatments. Individual measurements of $R_{area}^{25}$ showed a similar inverse relationship with mean daily air temperature across all salinity treatments. We conclude that photosynthetic responses to seasonal changes in temperature and *D*, as well as seasonal temperature acclimation of leaf *R*, are largely consistent across a range of salinities in *A. germinans*. These results might simplify predictions of photosynthetic and respiratory responses to temperature in young mangroves.

**Key words:** carbon assimilation, blue carbon, halophytes, salinity, stomatal sensitivity, thermal acclimation, vapor pressure deficit

## Introduction

Coastal ecosystems are increasingly recognized as important contributors in the global C cycle (Donato et al. 2011, McCleod et al. 2011, Duarte et al. 2013, Atwood et al. 2017). Ecosystems dominated by mangroves (tropical and subtropical woody halophytes) often have high rates of primary production (400 to 1200 g C $m^{-2}$ $y^{-1}$, 0.05 to 0.2 Pg C $yr^{-1}$ globally; Bouillon et al. 2008, Duarte et al. 2013, Alongi 2014, Duarte 2017). These ecosystems sometimes have higher rates of productivity than upland tropical forests when compared at a common height (Komiyama et al. 2008). Nonetheless, there remains considerable uncertainty about the physiological processes that regulate mangrove productivity (Bouillon et al. 2008, Krauss et al. 2008, Bauer et al. 2013, Alongi 2014), and how those processes vary over space and time and in response to changing environmental conditions.

Temperature is a key determinant of the extent and productivity of mangroves (Duke et al. 1998). Mangroves are generally intolerant of freezing and species range limits are strongly determined by the frequency of cold extremes. In fact, recent (30 to 50 yr) declines in cold extremes have contributed to the poleward movement of mangroves in many regions (Osland et al. 2013, Cavanaugh et al. 2014; 2018, Saintilan et al. 2014). Like other plants, temperature also mediates aspects of mangrove physiology; namely rates of leaf C fixation (i.e. photosynthesis, *A*) and respiration (*R*) (i.e. measured as $CO_2$ efflux). Photosynthesis and *R* regulate plant growth and ecosystem C storage, and at the global scale represent the two largest fluxes of C between vegetation and the atmosphere (Prentice et al. 2001, Canadell et al. 2007, IPCC 2013). Net photosynthesis (gross photosynthesis – *R*) is co-limited by diffusion of $CO_2$ through stomata, and by the

concentration and activity of photosynthetic enzymes. Stomatal sensitivity to temperature and vapor pressure deficit ($D$), as well as demand for $CO_2$, largely determine stomatal limitations to $A$. The maximum carboxylation rate of Rubisco ($V_{cmax}$) and the maximum rate of electron transport required to regenerate RuBP ($J_{max}$) are the primary biochemical determinants of $A$ (Farquhar et al. 1980). Leaf $R$ is primarily limited by the capacity of respiratory enzymes and the supply of carbohydrates produced by photosynthesis. Temperature directly influences rates of $A$ and $R$ by affecting the activity of photosynthetic and respiratory enzymes. Photosynthesis (as well as $V_{cmax}$ and $J_{max}$) and $R$ increase with increasing measurement temperature before reaching an optimum, after which they decline as temperature increases.

Short-term temperature response curves and diurnal gas-exchange measurements have indicated that the temperature optimum ($T_{opt}$) of $A$ in mangroves is between 25 and 32° C (Andrews and Muller 1985, Ball 1988, Ball et al. 1988, Cheeseman et al. 1997, Reef et al. 2016). However, there is little or no information on the response of leaf gas-exchange ($A_{sat}$, $g_s$), photosynthetic capacity ($V_{cmax}$ and $J_{max}$), or $R$ to seasonal changes in temperature or $D$ in mangroves (Krauss et al. 2008). The $T_{opt}$ (short- or long-term) of $V_{cmax}$ and $J_{max}$ has not been reported for any mangrove species. In other species, the $T_{opt}$ of $V_{cmax}$ is between 35 and 50 °C, and the $T_{opt}$ of $J_{max}$ is slightly lower (25 and 45 °C, Kattge and Knorr 2007, Kumarathunge et al. 2019). Likewise, thermal acclimation of leaf physiology can alter the temperature sensitivity of leaf $CO_2$ exchange (Atkin and Tjoelker 2003, Way and Yamori 2014). Most land plants acclimate to increasing temperature by increasing the $T_{opt}$ of $A$, $V_{cmax}$, and $J_{max}$ (Kattge and Knorr 2007, Kumarathunge et al. 2019) while decreasing rates of $R$ at a common temperature (e.g. Slot and Kitajima 2015, Aspinwall et al. 2016). Thermal acclimation of leaf physiology has not been widely studied in mangroves (but see Akaji et al. 2019). These knowledge gaps are important

given that land surface models, which are the basis of earth system models that predict future climate, project changes in $A$ (particularly $V_{cmax}$ and $J_{max}$), $R$, as well as C and N cycling, based directly on temperature changes (e.g. Community Land Model (CLM 5.0, Lawrence et al. 2019)). Furthermore, models that account for thermal acclimation of leaf $CO_2$ exchange predict greater terrestrial C storage in the future than models that do not (Lombardozzi et al. 2015, Smith et al. 2016). New examinations of mangrove photosynthetic and respiratory responses to temperature will improve our understanding of coastal C cycling and its contribution to the global C cycle.

Mangrove habitats also exhibit considerable spatial and temporal variability in nutrient inputs, tidal inundation, and salinity (Ball 1988, Duke et al. 1998, Krauss et al. 2008), all of which may interact with temperature and $D$ to impact leaf $CO_2$ exchange and productivity. Salinity effects can be particularly strong. Most mangroves grow best with some salt but salinity levels beyond species-specific thresholds can increase xylem tension, reduce growth, alter C allocation to leaves and roots, and reduce $g_s$ and $A$ (Clough and Sim 1982, Ball 1988, Smith et al. 1989, Ball and Pidsley 1995, Ball 2002, Reef et al. 2015a). However, salinity effects on mangrove photosynthetic biochemistry and $R$ remain understudied. Leaf $R$ sometimes increases at very high salinity presumably due to metabolic costs associated with maintaining intercellular ion gradients (Burchett et al. 1989, López-Hoffman et al. 2007). Potential interactions among salinity and temperature and $D$ are unclear but may be similar to interactions between light and salinity, where high salinity reduces mangrove $A$ at high light but has minimal effects at low light (López-Hoffman et al. 2007). High salinity might reduce $A$ more at high temperatures and high $D$, where stomatal limitations are high, photosynthetic inhibition is more likely, and

metabolic demands are already high. New studies are required to test whether mangrove photosynthetic and respiratory responses to temperature vary with salinity.

The goal of this study was to determine seasonal responses of leaf physiology (photosynthesis, respiration) to seasonal changes in temperature and *D* in black mangrove (*Avicennia germinans*), and the potential modifying effects of salinity. We accomplished this by growing *A. germinans* seedlings in an outdoor experiment at the species northern range limit for ~12 months under four salinity treatments spanning fresh water to hypersaline water (0 to 55 ppt porewater salinity). We repeatedly measured seedling growth and rates of $A$, $g_s$, $V_{cmax}$, and $J_{max}$ at prevailing leaf temperatures throughout the experiment, as well as rates of $R$ at a common temperature (25 °C). Salinity effects on biomass production and allocation were quantified at the end of the experiment. We then developed empirical models describing physiological responses to temperature and *D* across seasons, and changes in $R$ (at 25 °C) in response to mean daily air temperature and tested the effect of salinity on model parameters. We addressed four questions: 1) How do *in situ* rates of $A$ and $g_s$ respond to temperature and *D* across seasons? 2) How does photosynthetic capacity ($V_{cmax}$ and $J_{max}$) respond to seasonal temperature changes? 3) Is there evidence of seasonal temperature acclimation of leaf $R$? and 4) Does salinity alter *in situ* gas-exchange ($A_{sat}$, $g_s$) responses to temperature and *D*, photosynthetic capacity responses to seasonal temperature change, or seasonal temperature acclimation of leaf $R$? We hypothesized that increasing salinity would compound reductions in $A$ and $g_s$ at high temperatures and would limit declines in leaf $R$ (at 25 °C) with increasing temperature (i.e. thermal acclimation) due to increased metabolic demands.

## Materials and methods

### *Plant material and experimental design*

*Avicennia germinans* is a broadly distributed mangrove species native to warm-temperate, subtropical, and tropical regions of the Americas and Africa. On the Pacific coast, its distribution stretches from Mexico to Peru. On the Atlantic coast, its distribution stretches from North Florida to southern Brazil. The species grows under a wide range of salinity conditions, although productivity tends to decline above porewater salinities of 20-35 ppt (Suárez and Medina 2006, Dangremond et al. 2015). In October 2017 roughly 150 propagules of *A. germinans* were collected off the beach at Fort Clinch on Amelia Island, FL, USA (30.6701° N, 81.4346° W). This location represents the species northern range limit and is close to the site of the experiment. The source tree(s) and geographic origin of the propagules are unknown, yet these propagules are representative of the germplasm that would become established at the species northern range limit.

Propagules were collected and rooted in small containers (Ray Leach Cone-tainers, Stuewe and Sons Inc., Tangent, OR, USA) filled with a 2:1 mixture of potting soil and sand. Propagules were grown in walk-in growth chambers (night/day air temperature = 16°C/27 °C, 16-hr light period at 300 µmol $m^{-2}$ $s^{-1}$ photosynthetically active radiation) at the Smithsonian Environmental Research Center in Edgewater, MD, USA for 2-3 months before being transferred to a naturally lit glasshouse facility at the University of North Florida (UNF) in Jacksonville, FL, USA (30.2661° N, 81.5072° W) on 25 January 2018. By this time, the propagules had grown into seedlings (~15 cm tall, 4-6 leaves). On 13 April 2018, seedlings had roughly doubled in size. Thirty-six seedlings were identified that were of average size, based on stem diameter (at 5 cm

above the root collar, 4.2 ± 0.6 (standard deviation) mm), stem length (33.0 ± 6.2 cm), and number of leaves (12 ±1.7 leaves). Each seedling was planted in a separate 56 L fabric root pouch (Root Pouch, Hillsboro, OR, USA) filled with commercial garden soil composed of ~ 80% organic matter and ~20% sand (Sta-Green Garden Soil, Rowlett, TX, USA). The soil contained a slow release fertilizer such that total soil N, P, and K concentrations were 500 mg $kg^{-1}$, 500 mg $kg^{-1}$, and 30 mg $kg^{-1}$, respectively.

Root pouches containing individual seedlings were moved to a small (~56 $m^2$) outdoor sun-lit location on the UNF campus on 3 May 2018. The study was carried out using a randomized complete block design, with four salinity treatments replicated nine times (*n*=36 seedlings). Each seedling was placed in an individual 121 L plastic container. Containers were arranged in nine blocks of four, with each salinity treatment randomly assigned to one container in each block. Blocks were spaced roughly 1.5 m apart in a 3 × 3 grid (see Figure S1). Root pouches were placed inside each container such that the edge of the root pouch was just below the edge of the container. Initially, fresh (tap) water was added to each container. Then, over one week we gradually increased porewater salinity from 0 to 18 ppt in containers designated to receive one of the salinity treatments. This was done to avoid salt shock. Salinity treatments officially began 12 June 2018. We implemented four treatments representing the range of porewater salinities in mangrove habitats: freshwater (FW, 0 ppt), brackish (BW, 18 ppt), seawater (SW, 35 ppt) and hypersaline (HS, 55 ppt). Salinity levels were achieved by mixing salt (Instant Ocean Sea Salt, Blacksburg, VA, USA) with freshwater inside large (208 L) drums and adding water with the target salinity levels to the designated treatment containers. We monitored salinity concentrations on a weekly basis using a handheld salinity sensor (YSI Model 85, YSI Incorporated, Yellow Springs, OH, USA) and added new water containing the target salinity as

needed. Salinity concentrations were never more than 2-3 ppt higher or lower than target levels. When precipitation caused water levels to inundate seedlings, we removed water with a siphon pump and added water of the target salinity as needed, ensuring that water levels were flush with the soil surface. Although tidal changes cause water levels to fluctuate in mangrove habitats, we were unable to simulate this in our design and chose to maintain constant water levels over time and across treatments. Air temperature and relative humidity (RH) at the site were measured every 15 minutes with an air temperature/RH sensor (Model US23 Pro v2, HOBO Instruments Inc., Bourne, MA, USA). The average daily air temperature over the course of the experiment was 22 °C (Figure S2), which is higher than the long-term (1981 – 2010) mean annual temperature at this location (20 °C, NOAA). Daily mean air temperature during summer (June – August) was between 25 and 30 °C (Figure S2), with maximum air temperatures near 35 °C. Daily mean air temperatures during winter (December – February) varied between 10 and 20 °C, with minimum temperatures dropping below 0 °C on two dates. The average daily relative humidity was 82%, and the mean maximum and minimum relative humidity was 98% and 55%, respectively (Figure S2).

***Leaf photosynthesis***

We measured the $CO_2$ response of leaf-level net photosynthesis on one leaf of 3-6 seedlings in each salinity treatment at seven timepoints (one pretreatment timepoint, six timepoints during treatments) using two portable photosynthesis systems (LI-6800 or LI-6400XT, LiCor., Inc, Lincoln NE, USA). We also measured $CO_2$ responses of net photosynthesis on 1-2 seedlings of each salinity treatment at two additional timepoints, both of which were the coolest timepoints during the experiment. Fewer photosynthetic $CO_2$ response measurements were possible at the

coolest timepoints (i.e. winter) because most seedlings showed very low rates of stomatal conductance, hindering our ability to measure the $CO_2$ response of photosynthesis. Data collected at these timepoints were excluded from statistical tests of the main and interactive effects of measurement date and salinity on biochemical parameters of photosynthesis but were included in empirical models describing the seasonal temperature response of photosynthetic biochemistry.

For all photosynthetic measurements, the LI-6400XT was fitted with a 2 x 3 cm cuvette head while the LI-6800 was fitted with a 3 x 3 cm cuvette head; both cuvettes were fitted with a red and blue LED light source. Measurements were made on recently mature, fully expanded, upper canopy leaves. When leaves did not fill the cuvette, we used a ruler to estimate leaf area inside the cuvette (based on leaf width and length) and back-corrected the gas-exchange data accordingly. Measurements occurred between 10:00 and 14:00 local time. Leaves were acclimated to ambient temperature conditions and a constant photosynthetic photon flux density (PPFD) of 1500 μmol $m^{-2}$ $s^{-1}$ before beginning measurements of the $CO_2$ response of photosynthesis. Net photosynthesis in *A. germinans* seedlings has been shown to saturate at 1500 μmol $m^{-2}$ $s^{-1}$ PPFD (Krauss et al. 2006). Flow rate was held constant at 500 μmol $s^{-1}$. Leaf temperature ($T_{leaf}$) was measured with the built-in leaf temperature thermocouple. Relative humidity conditions in the chamber were controlled near ambient external conditions, but also varied depending upon water vapor fluxes from the leaf. Thus, vapor pressure deficit conditions at the leaf surface varied over time. Each $CO_2$ response measurement began with steady-state measurements of light-saturated net photosynthesis ($A_{sat}$, μmol $m^{-2}$ $s^{-1}$), stomatal conductance to water vapor ($g_s$, mol $m^{-2}$ $s^{-1}$), intercellular $CO_2$ concentration ($C_i$), and atmospheric $CO_2$ ($C_a$) at a chamber reference [$CO_2$] of 420 μmol $mol^{-1}$. Leaves typically reached steady-state within 5-10

minutes of being enclosed in the cuvette. The ratio of $C_i/C_a$ represents the balance between $CO_2$ diffusion into the leaf (regulated by $g_s$) and $CO_2$ fixation by photosynthesis. High $C_i/C_a$ indicates low $A_{sat}$ relative to $g_s$ (low intrinsic water use efficiency) and low $C_i/C_a$ indicates high $A_{sat}$ relative to $g_s$ (high intrinsic water use efficiency).

Measurements of the $CO_2$ response of photosynthesis were produced by measuring $A_{sat}$ at a series of reference [$CO_2$]: 300, 250, 100, 50, 0, 420, 650, 800, 1200, and 1500 μmol $mol^{-1}$. $C_i$ was recorded at each reference [$CO_2$] and photosynthetic $CO_2$ response measurements were constructed by examining relationships between $A_{sat}$ and $C_i$. We also recorded steady state measurements of $A_{sat}$, $g_s$, and $C_i/C_a$ on of 3-6 seedlings of each salinity treatment at three additional timepoints. In total, *in situ* measurements of $A_{sat}$, $g_s$, and $C_i/C_a$ were made at 10 timepoints (after salinity treatments began).

Each photosynthetic $CO_2$ response measurement was parameterized using the Farquhar model of $C_3$ photosynthesis (Farquhar et al. 1980). The model estimates the maximum rate of Rubisco carboxylation ($V_{cmax}$; μmol $m^{-2}$ $s^{-1}$) and the rate of electron transport for RuBP regeneration ($J_{max}$; μmol $m^{-2}$ $s^{-1}$). The model was fit using non-linear regression in SAS v9.3 (PROC NLIN, SAS Institute Inc., 2010). In total, we calculated 148 estimates of both $V_{cmax}$ and $J_{max}$ across a seasonal temperature range of 10 to 35 °C. We used these data to calculate the ratio of $J_{max}$ to $V_{cmax}$ ($J_{max}/V_{cmax}$) which provides information about resource allocation to the light- versus carbon-limiting processes of photosynthesis.

The seasonal temperature response of $A_{sat}$, $g_s$, $V_{cmax}$ and $J_{max}$ all showed evidence of a peaked temperature response. We compared the fit of several models that might describe the peaked temperature response of each variable. Models were parameterized using nonlinear regression with the Levenberg–Marquardt algorithm for minimizing the error sum of squares

(PROC NLIN, SAS Institute Inc. 2010). For $A_{sat}$ and $g_s$, we compared the fits of a parabola (see Battaglia et al. 1996) and two empirical functions; a cubic function, and a 4-parameter log-normal function in the form:

Equation 1 $$y = y_0 + a/T_{leaf} \times e[-0.5(ln(T_{leaf}/x_0)/b)^2]$$

where $y_0$ is the intercept, $x_0$ estimates the $T_{leaf}$ at which $A_{sat}$ and $g_s$ are maximal (i.e. temperature optimum), and $a$ and $b$ parameters that describe the shape of the temperature response. For $V_{cmax}$ and $J_{max}$ we compared the fits of the peaked Arrhenius equation (Medlyn et al. 2002), the 4-parameter log-normal function (Equation 1), and a cubic function. The 4-parameter log normal function (Equation 1) provided the best fit for all variables; we found strong linear relationships between observed and predicted values (obs $A_{sat}$ vs pred $A_{sat}$, $r^2$=0.60, $P$<0.0001; obs $g_s$ vs pred $g_s$, $r^2$=0.47, $P$<0.0001; obs $V_{cmax}$ vs pred $V_{cmax}$, $r^2$=0.63, $P$<0.0001; obs $J_{max}$ vs pred $J_{max}$, $r^2$=0.55, $P$<0.0001), and residuals were normally distributed around zero with little pattern associated with increasing $T_{leaf}$. Thus, we used this empirical function for describing the temperature response of $A_{sat}$, $g_s$, $V_{cmax}$ and $J_{max}$.

A linear function was used to describe the relationship between $C_i/C_a$ and $T_{leaf}$, and $C_i/C_a$ and $D$. The relationships between $A_{sat}$ and $D$, and $g_s$ and $D$ were described by a linear function in the form: $g_s = -m \cdot ln(D) + b_{ref}$, where $m$ quantifies the sensitivity of $A_{sat}$ or $g_s$ to increasing $D$ (μmol $m^{-2}$ $s^{-1}$ $ln$(kPa)$^{-1}$ or mol $m^{-2}$ $s^{-1}$ $ln$(kPa)$^{-1}$) and $b_{ref}$ is the reference $A_{sat}$ or $g_s$ at $D$ = 1 kPa (Oren et al. 1999). All models described above were fit using pooled data for each salinity treatment so that salinity effects on model parameters could be examined as described in the Data Analysis section below.

***Leaf respiration***

Measurements of night-time leaf *R* per unit area ($R_{area}$, μmol $m^{-2}$ $s^{-1}$) were taken at nine timepoints after the start of salinity treatments. Measurements carried out the same day or a few days after measurements of $A_{sat}$ were carried out on the same leaves (which were tagged), as well as two other leaves of similar age and canopy position. Measurements carried out at timepoints that did not coincide with photosynthetic $CO_2$ responses or $A_{sat}$ measurements were made on three randomly chosen leaves of similar age and canopy position. Measurements of *R* were made on excised leaves collected two hours after sunset. Sampling of leaves from different salinity treatments occurred randomly within and across dates. After excision, leaves were taken to a temperature-controlled room set to approximately 25 ºC. Rates of *R* were measured by placing leaves from each seedling in a large gas-exchange chamber (LI-6400-22L or LI-6800-24, LI-COR, Inc.), which increased $CO_2$ differentials (sample $CO_2$ – reference $CO_2$) without leak artifacts (Jahnke and Krewitt 2002, Drake et al. 2015). Reference [$CO_2$] was fixed at 410 μmol $mol^{-1}$. Leaf area ($cm^2$) of the measured leaves was determined with a leaf area meter (CI-202 Portable Leaf Area Meter, CID Instruments) just prior to measurements of leaf *R* and was used to correct measurements of *R* per unit area. Repeated measurements of leaf *R* at a set temperature of 25 °C ($R_{area}^{25}$) provide a direct measure of the degree of seasonal temperature acclimation of leaf *R*. If seasonal temperature acclimation of leaf *R* is occurring, we expect an inverse relationship between prevailing mean daily temperatures and $R_{area}^{25}$. The slope of the relationship indicates the strength of acclimation. Following measurements of leaf $R_{area}^{25}$, leaves were placed in envelopes and dried at 70 °C for 72 hrs. Leaf dry mass per unit area (LMA, g $m^{-2}$) of the gas-exchange leaves was calculated as the ratio of leaf dry mass (g) to leaf area multiplied by 0.0001.

***Plant growth and biomass allocation***

Stem diameter (*d*) and stem length (*l*) were measured on each seedling at 22 timepoints between 13 April 2018 and 20 May 2019. At each timepoint, stem diameter was measured at 5 cm above the root collar with digital calipers. Stem length was measured with a ruler. Stem *d* and *l* were used to estimate the volume of the main stem (*V*, $cm^3$) based on the volume of cone ($V = \pi \times (d/2)^2 \times (l/3)$).

Seedlings were harvested on 20 May 2019, almost a year after the salinity treatments began. The stem of each seedling was cut at the soil surface and the aboveground portion was separated into stem, branches, and leaves. Stem and branch material was dried at 70 °C for seven days, and weighed to determine stem and branch dry mass (Stem DM and Branch DM, respectively). All leaves of each seedling were immediately weighed to determine total leaf fresh mass. A random subsample of 25 leaves were collected from each seedling and subsample fresh mass was determined. We determined the area ($cm^2$) of the subsampled leaves using a portable leaf area meter (CI-202 Portable Leaf Area Meter, CID Instruments), and dried the subsampled leaves at 70 °C for three days to determine moisture content. Specific leaf area (SLA, $cm^2\ g^{-1}$) was estimated by dividing subsample leaf area by dry mass. Total leaf dry mass (Leaf DM) was estimated by multiplying the subsample dry matter content (dry mass/fresh mass) by total leaf fresh mass. Total leaf area ($m^2$) was estimated by multiplying subsample SLA ($m^2\ g^{-1}$) by the estimate of leaf DM. The entire belowground portion was washed free of soil and dried at 70 °C for seven days to determine total root dry mass (Root DM). Total tree dry mass (Total DM) was calculated by summing Stem DM, Branch DM, Leaf DM, and Root DM. Allocation to different biomass pools, relative to Total DM, was determined for each plant by calculating leaf mass fraction (LMF, $g\ g^{-1}$), stem mass fraction (SMF, main stem + branches, $g\ g^{-1}$), and root mass

fraction (RMF, g $g^{-1}$). Leaf area ratio (LAR, $cm^2$ $g^{-1}$) was calculated as the ratio of total leaf area to Total DM.

***Data analysis***

All statistical analyses were performed in SAS v9.3 (SAS Institute Inc. 2010). All tests of statistical significance were conducted at $\alpha = 0.05$. Mixed-effect models were used to test the fixed effects of time (measurement date), salinity treatment (FW, BW, SW, HS) and their interaction on seedling stem volume, $A_{sat}$, $g_s$, $C_i/C_a$, $V_{cmax}$, $J_{max}$, $J_{max}/V_{cmax}$, and $R_{area}^{25}$. Because seedlings were repeatedly sampled over time, we fit a random intercept term for the effect of seedling within salinity treatment. Mixed-effect models were also used to test the fixed effects of salinity on seedling biomass production (e.g. Total DM, Leaf DM) and biomass allocation (e.g. SMF, RMF, LAR), with block considered a random effect.

Analysis of covariance was used to test for salinity effects on parameters of the linear function describing the seasonal temperature response of $C_i/C_a$, the ratio of $J_{max}/V_{cmax}$, and $R_{area}^{25}$, as well as the response of $A_{sat}$, $g_s$, and $C_i/C_a$ to $D$. When salinity effects were not significant, a single function was fit to the data.

We tested salinity effects on the long-term temperature response of $A_{sat}$, $g_s$, $V_{cmax}$, and $J_{max}$ by examining whether 95% confidence intervals for the estimated temperature response parameters overlapped among salinity treatments. For each salinity treatment, we calculated upper and lower 95% confidence intervals for each parameter by multiplying the standard error of the parameter estimate by 1.96 (critical value when $\alpha = 0.05$). When confidence intervals of parameters overlapped among treatments, we concluded that salinity effects on the long-temperature response were not significant.

## Results

### *Growth and biomass allocation*

Salinity effects on stem volume varied over time (date × salinity interaction, Figure 1). Stem volume was not significantly different among treatments until five months after the start of salinity treatments (November 2018), after which BW and SW seedlings showed increasingly higher stem volume than FW and HS seedlings (Figure 1).

Leaf DM, Stem DM, Branch DM and Total DM were significantly higher in BW and SW seedlings than FW and HS seedlings (Table 1). Root DM was significantly lower in FW seedlings compared to BW and SW seedlings (Table 1). Salinity had no significant effect on biomass allocation (Table 1). Total tree LA was significantly higher in the BW and SW seedlings compared to the FW and HS seedlings. LAR and SLA were generally higher in BW, SW, and HS seedlings than FW seedlings (Table 1).

### *Seasonal temperature response of photosynthesis and stomatal conductance*

A weak date × salinity interaction was observed for $A_{sat}$ and $g_s$ (Table 2) driven by a single measurement date (23 August 2018) where FW seedlings showed 204% higher $A_{sat}$ and 259% higher $g_s$ than HS seedlings ($P$<0.01 and $P$=0.02, respectively, Figure 2a and 2b). $A_{sat}$ and $g_s$ did not differ among salinity treatments on any other measurement date. $C_i/C_a$ varied over time but was not affected by salinity (Table 2, Figure 2c).

Salinity had little or no effect on the parameters describing the seasonal temperature response of $A_{sat}$ and $g_s$ (Table 2). In nearly all cases, 95% confidence intervals for parameter estimates overlapped across treatments (Figure S3). The only exception was for the model

describing the relationship between $g_s$ and $T_{leaf}$. Parameter *b*, which describes the shape of temperature response but is not readily interpretable, was significantly higher in the HS seedlings compared to FW, BW, and SW seedlings (Figure S3). The remaining parameters ($a$, $x_0$, and $y_0$) describing the relationship between $g_s$ and $T_{leaf}$ were similar among salinity treatments (Figure S3). Given that model parameters were largely similar among salinity treatments, data were pooled and a single function was used to describe seasonal temperature responses of these variables (Table 3, Figure 2d,e). Peak rates of $A_{sat}$ and $g_s$ occurred at leaf temperatures between 29 and 30 °C. At $T_{leaf}$ = 29 °C, average rates of $A_{sat}$ and $g_s$ were roughly 19 μmol $CO_2$ $m^{-2}$ $s^{-1}$ and 0.28 mol $H_2O$ $m^{-2}$ $s^{-1}$, respectively (Figure 2d,e). However, at any given leaf temperature, measurements of $A_{sat}$ and $g_s$ varied considerably among individual leaves. This variation was primarily explained by the close coupling of these two processes; $A_{sat}$ increased with increasing $g_s$ and vice versa (Figure S4).

The relationship between *D* and individual measurements of $A_{sat}$ and $g_s$ was variable (Figure 2g,h). $A_{sat}$ and $g_s$ measurements taken at low *D* (< 1 kPa) and low $T_{leaf}$ (< 20 °C) were low and did not fit the trajectory of $A_{sat}$ and $g_s$ data collected at higher *D* and $T_{leaf}$ (Figure 2g,h). For simplicity, we fit the model of Oren et al. (1999) to $A_{sat}$ and $g_s$ data collected at $T_{leaf}$ > 20 °C only. Salinity had no effect on the relationship between $A_{sat}$ and *D* (intercept, *P*=0.93; slope, *P*=0.62) and $g_s$ and *D* (intercept, *P*=0.88; slope, *P*=0.75). Across salinity treatments, the reference $A_{sat}$ and $g_s$ at *D* = 1 kPa was 19.8 ± 1.1 μmol $m^{-2}$ $s^{-1}$ and 0.30 ± 0.02 mol $m^{-2}$ $s^{-1}$, respectively (Figure 2g,h). The sensitivity of $A_{sat}$ and $g_s$ to increasing *D* was -9.34 ± 1.6 μmol $m^{-2}$ $s^{-1}$ $ln$(kPa)$^{-1}$ and -0.178 ± 0.03 mol $m^{-2}$ $s^{-1}$ $ln$(kPa)$^{-1}$, respectively (Figure 2g,h). Salinity had no effect on the relationship between $C_i/C_a$ and

$T_{leaf}$ (intercept, $P$=0.37; slope, $P$=0.58) and $C_i/C_a$ and $D$ (intercept, $P$=0.39; slope, $P$=0.51; Figure 2f,i). We conclude that leaf gas-exchange responses to seasonal changes in $T_{leaf}$ and $D$ did not differ among salinity treatments.

A weak date × salinity interaction was observed for $V_{cmax}$ and $J_{max}$ (Table 2), but after adjusting for multiple comparisons, $V_{cmax}$ and $J_{max}$ did not differ among treatments on any individual date (Figure 3a,b). Excluding measurements taken before salinity treatments began, the seasonal temperature response of $V_{cmax}$, $J_{max}$, and $J_{max}/V_{cmax}$ was similar among salinity treatments; 95% confidence intervals for model parameters overlapped of each salinity treatment (Table 3, Figure S3). Averaged across treatments, peak rates of $V_{cmax}$ occurred at higher $T_{leaf}$ (36 °C) than peak rates of $J_{max}$ (30 °C, Table 3, Figure 3d,e). The intercept parameter of the temperature response function provided an estimate of $V_{cmax}$ and $J_{max}$ at the lowest measurement $T_{leaf}$ (~11 °C). At this $T_{leaf}$, $V_{cmax}$ and $J_{max}$ averaged 28 μmol $m^{-2}$ $s^{-1}$ and 76 μmol $m^{-2}$ $s^{-1}$, respectively, across salinity treatments (Table 3, Figure 3d,e). The ratio of $J_{max}/V_{cmax}$ declined linearly as $T_{leaf}$ increased (Figure 3f) indicating that $CO_2$-limited processes increased more as seasonal temperatures increased relative to light-limited photosynthetic processes.

***Respiratory responses to seasonal temperature changes***

A date × salinity interaction was observed for $R_{area}^{25}$ (Table 1). After adjusting for multiple comparisons, $R_{area}^{25}$ only differed among salinity treatments on the last measurement date (2 May 2019). On this date, $R_{area}^{25}$ was 82-96% higher in BW, SW, and HS seedlings than FW seedlings (Figure 4a). Despite this interaction, the slope and intercept parameters describing the relationship between individual measurements of $R_{area}^{25}$ and prevailing 5-day mean temperature did not differ between salinity treatments (intercept, $P$=0.72, slope, $P$=0.85). Thus, seedlings of

all treatments showed a general acclimation response to increasing seasonal temperatures demonstrated by a reduction in $R_{area}^{25}$ ($r^2$ = 0.20, Figure 4b).

## Discussion

We tested whether salinity alters physiological (photosynthetic, respiratory) responses of black mangrove (*Avicennia germinans*) to seasonal changes in temperature and *D*. Over time, salinity had weak or inconsistent effects on $A_{sat}$ and $g_s$. Moreover, salinity had no effect on the biochemical parameters of photosynthesis ($V_{cmax}$, $J_{max}$) and individual measurements of $A_{sat}$, $g_s$, $V_{cmax}$, and $J_{max}$ showed a similar response to seasonal changes in $T_{leaf}$ and *D* across all salinity treatments. Despite a significant date × salinity interaction driven by one measurement date, individual measurements of $R_{area}^{25}$ showed a similar inverse relationship with mean daily air temperature across all salinity treatments. We conclude that photosynthetic responses to seasonal changes in temperature and *D*, as well as seasonal temperature acclimation of leaf *R*, are largely consistent across a range of salinities in *A. germinans* seedlings. These results might simplify predictions of photosynthetic and respiratory responses to temperature in young mangroves.

### *Photosynthetic responses to temperature and D*

We hypothesized that increasing salinity would cause larger reductions in $A_{sat}$ at high temperatures and high *D* rather than cool temperatures and low *D* due to stomatal limitation of $CO_2$ diffusion (lower $g_s$), potential temperature-inhibition of photosynthetic enzymes, and the potentially compounding effects of high salinity and high temperature on leaf metabolism. In contrast to our hypothesis, we found that parameters describing the seasonal response of $A_{sat}$ to temperature and *D* did not differ among salinity treatments. In particular, the long-term $T_{opt}$ of

$A_{sat}$ was 29-30 °C in all treatments, which is within the $T_{opt}$ range for mangroves reported by other studies (e.g. Ball 1988, Ball et al. 1988, Reef et al. 2016). Weak or inconsistent effects of salinity on $A_{sat}$ over time may help explain the convergence in the seasonal response of $A_{sat}$ to temperature and $D$ across salinity treatments. Previous studies have found inconsistent effects of high salinity on $A_{sat}$ in *A. germinans*. Some studies have shown substantial reductions in $A_{sat}$ with increasing salinity (Sobrado 1999, Suárez and Medina 2006) while others have reported little change in $A_{sat}$ across a broad range of salinities (Pezeshki et al. 1990, Lovelock and Feller 2003).

Weak or inconsistent effects of salinity on $A_{sat}$ and the convergent response of $A_{sat}$ to temperature and $D$ across salinity treatments may be partly explained by weak or inconsistent effects of salinity on $g_s$. Previous studies that have demonstrated reductions in $A_{sat}$ with increasing salinity in *A. germinans* and other mangroves have observed similar (or larger) reductions in $g_s$, indicating strong stomatal limitation of photosynthesis (Clough and Sim 1982, Smith et al. 1989, Suárez and Medina 2006, Reef et al. 2015a). We also found that $A_{sat}$ and $g_s$ are closely coupled across salinity treatments and over time (Figure S4). As such, small effects of salinity on $g_s$ paralleled small effects of salinity on $A_{sat}$, resulting in a common response of both parameters to temperature and $D$. The close coupling of $A_{sat}$ and $g_s$ also resulted in a nearly constant ratio of $C_i/C_a$ among salinity treatments, and a convergent response of $C_i/C_a$ to temperature and $D$. We note that estimated rates of $g_s$ at 1 kPa $D$ (i.e. $b_{ref}$) and stomatal sensitivity to $D$ ($m$) in our study are relatively similar to estimates of $b_{ref}$ and $m$ in other terrestrial broadleaved evergreen species (Körner and Cochrane 1985, Oren et al. 1999, Cunningham 2004). Understanding mangrove stomatal sensitivity to $D$ and resulting impacts on mangrove carbon and water fluxes will likely become more important as the planet warms and $D$ increases (Novick et al. 2016).

It is somewhat surprising that increasing salinity had little effect on $g_s$, given that xylem tension typically increases at high salinity (Smith et al. 1989, Suárez and Medina 2006, Krauss et a. 2008) which should result in reduced $g_s$. We did not measure leaf water potential, so it is unclear how the small reductions in $g_s$ relate to changes in leaf water potential. However, *A. germinans* is known to adjust to high salinity by accumulating inorganic ions ($Na^+$, $K^+$) in the vacuole and organic compounds (glycinebetaine, mannitols, proline) in non-vacuolar regions (Popp 1995, Krauss et al. 2008, Parida and Jha 2010), which can help reduce xylem tension and allow for water uptake and turgor maintenance at high salinity (Suárez et al. 1998, Sobrado and Ewe 2006). It is likely that long-term and constant exposure to high salinity resulted in osmotic adjustment that may have mitigated the impacts of high salinity on $g_s$ and $A_{sat}$. Indeed, rates of $A_{sat}$ and $g_s$ in the HS treatment declined strongly following the start of salinity treatments (~2 months), but subsequently increased and were comparable to rates in the remaining treatments throughout the rest of the study, which may reflect salt acclimation. Moreover, acclimation to constant salinity levels may demand less energy than acclimation to fluctuating salinity, which could result in relatively similar gas-exchange over time (Lin and Sternberg 1993, Bompy et al. 2014). It is also possible that seedlings adjusted to high salinity by increasing leaf cell rigidity which may enable higher cellular water content, a lower turgor loss point, and perhaps rates of leaf gas-exchange equivalent to those of seedlings grown under moderate salinity (Nguyen et al. 2017). A different study would be required to test the effects of fluctuating salinity treatments versus near-constant salinity treatments on mangrove physiological responses to temperature and *D*.

Large variation in $A_{sat}$ and $g_s$ among individual leaves might have also partly obscured salinity effects on leaf physiology. Availability of freshwater from rainfall, patchiness in salinity in the soil water surrounding roots, and patchiness in leaf salt concentrations might have contributed to variation in $A_{sat}$ and $g_s$ among the BW, SW, and HS seedlings (Reef and Lovelock 2015). Salinity is often variable within soil, and there is some evidence that mangroves can access and use less-saline pools of water, when available, which could result in maintenance of hydraulic function and leaf gas-exchange (Ewe et al. 2007, Lambs et al. 2008, Reef et al. 2015b). However, there was also considerable leaf-to-leaf variation in $A_{sat}$ and $g_s$ among FW seedlings that did not receive salt. Further studies are required to determine the source of this variation among mangrove leaves.

Salinity had little effect on $CO_2$-limited processes ($V_{cmax}$) and light-limited processes ($J_{max}$) of photosynthesis, and both parameters (and the ratio of $J_{max}/V_{cmax}$) showed consistent responses to seasonal temperature changes across all salinity treatments. Few studies have examined salinity effects on $V_{cmax}$ or $J_{max}$ in mangroves, but some have found similar results. For instance, López-Hoffman et al. (2007) also found that increasing salinity from 20% seawater (~7 ppt) to 167% seawater (~58 ppt) had no effect on $V_{cmax}$ in *A. germinans*. Ball and Farquhar (1984) found that transient increases in salinity reduced the initial slope of the $A$-$C_i$ relationship in *A. marina*, indicating a reduction in $V_{cmax}$, but this reduction was reversible when salinity subsequently declined. In contrast, Suárez and Medina (2006) found a ~50% reduction in $V_{cmax}$ in *A. germinans* when salinity increased from 0 to 55 ppt. Although more studies are required, it appears that mangrove photosynthetic biochemistry may be relatively insensitive to long-term differences in salinity.

The shape of the long-term temperature response of $V_{cmax}$ and $J_{max}$ was similar to short- and long-term temperature responses of $V_{cmax}$ and $J_{max}$ observed in many terrestrial non-halophyte species (Dreyer et al. 2002, Medlyn et al. 2002, Xu and Baldocchi 2003, Kosugi and Matsuo 2006, Crous et al. 2013, Aspinwall et al. 2017). $V_{cmax}$ and $J_{max}$ increased quasi-exponentially with increasing $T_{leaf}$ before reaching an optimum; 36 °C for $V_{cmax}$ and 30 °C for $J_{max}$. This result aligns with previous studies that have found that the $T_{opt}$ of $J_{max}$ is generally lower than the $T_{opt}$ of $V_{cmax}$ (Kattge and Knorr 2007, Kumarathunge et al. 2019). Interestingly, the long-term $T_{opt}$ of $J_{max}$ was ~1 °C higher than the $T_{opt}$ of $A_{sat}$ and $g_s$, which could indicate that the temperature threshold for $A_{sat}$ in *A. germinans* is jointly determined by stomatal limitations and biochemical limitations associated with electron transport for RuBP regeneration. The $T_{opt}$ of $J_{max}$ was also similar to the mean daily summer temperature at our site (~30 °C), and below the maximum summertime temperatures (Figure S2). This could indicate that RuBP regeneration was regularly inhibited during summer and may be increasingly inhibited as climate warms. However, many plants acclimate to changing temperatures by adjusting the $T_{opt}$ of photosynthetic parameters (Way and Yamori 2014, Kumarathunge et al. 2019). Measurements of the short-term temperature response of $A_{sat}$, $V_{cmax}$, and $J_{max}$ during different seasons are needed to more fully reveal the proximity of the $T_{opt}$ of photosynthesis to prevailing temperatures. Finally, *A. germinans* showed a strong linear decline in $J_{max}/V_{cmax}$ as leaf temperatures increased indicating that increasing seasonal temperatures stimulated $V_{cmax}$ more so than $J_{max}$, similar to observations in other $C_3$ plant species (Robakowski et al. 2002, Kattge and Knorr 2007, Smith and Dukes 2017).

***Respiration, salinity, and temperature***

Leaf *R* is expected to increase with increasing salinity due to metabolic demands associated with salt removal and maintenance of ion gradients (Krauss et al. 2008), but experimental evidence for salinity effects on mangrove leaf *R* is mixed (Burchett et al. 1989, López-Hoffman et al. 2007). We found that salinity had weak or inconsistent effects on leaf *R* (repeatedly measured at 25 °C, $R_{area}^{25}$) over time, although average $R_{area}^{25}$ increased slightly with increasing salinity, similar to the findings of López-Hoffman et al. (2007).

Despite a significant date × salinity interaction for $R_{area}^{25}$ we found no evidence that seasonal temperature acclimation of leaf *R* differed between salinity treatments. Thus, *A. germinans* growing under habitats that differ in salinity may show a common acclimation response to seasonal temperature changes, which could simplify predictions of the temperature sensitivity of respiratory carbon fluxes in mangroves. Even so, ~80% of the variation in individual measurements of $R_{area}^{25}$ was not explained by prevailing air temperature. Seedlings were grown under uniform light and nutrient conditions so the source of the unexplained variation remains unclear but could be explained by heterogeneity in salt excretion, leaf nitrogen, or carbohydrate accumulation among leaves within and among seedlings.

In our study the slope describing the change in $R_{area}^{25}$ with increasing air temperatures was -0.047. This is lower than the slope describing seasonal acclimation of leaf *R* in temperate-subtropical origin *Eucalyptus tereticornis* (-0.084, Aspinwall et al. 2016) and temperate *Fagus sylvatica* (~ -0.070, Rodríguez-Calcerrada et al. 2009). If $R_{area}^{25}$ is expressed on a mass basis ($R_{mass}^{25}$, data not shown), the slope describing seasonal acclimation of leaf *R* in our study was -0.28, which is higher than the slope describing seasonal acclimation of leaf *R* in a boreal needled evergreen species (-0.13, *Pinus banksiana*, Tjoelker et al. 2008, 2009), but is much lower than

the slope for seasonal acclimation of leaf *R* in temperate deciduous tree species (-1.1 to -1.5, Lee et al. 2005). Thus, *A. germinans*, a tropical-subtropical halophyte, may show weaker seasonal acclimation of leaf *R* than some terrestrial broadleaved tree species from cooler climates. However, this contrasts with Slot and Kitajima (2015) who found little difference in thermal acclimation of leaf *R* between species from different biomes. Further studies are required to determine whether mangroves acclimate differently to temperature changes compared to terrestrial species from different biomes.

***Salinity effects on growth and biomass allocation***

Biomass and leaf area production was optimal under BW and SW conditions, and lower under FW and HS conditions. These results align with previous studies in *A. germinans* and other mangroves (Ball 2002, Parida et al. 2004, Suarez and Medina 2006, López-Hoffman et al. 2006; 2007, Nguyen et al. 2015, Dangremond et al. 2016). Slightly higher average rates of $A_{sat}$ averaged across more leaf area could partially explain why BW and SW seedlings were more productive, although salinity effects on cell division and expansion might also explain salinity effects on total biomass production (West et al. 2004, Munns and Tester 2008).

Previous studies in *A. germinans* and other mangroves have generally found that allocation to roots increases with salinity, while allocation to leaves decreases with salinity (Ball 2002, López-Hoffman et al. 2006; 2007, Nguyen et al. 2015). Given that increasing salinity tends to increase xylem tension (i.e. water stress), this response is interpreted as strategy for increasing access and conservation of water. We also found slight increases in RMF with salinity, at the expense of SMF, but LMF did not change with salinity, and the overall effect of salinity on biomass fractions was not significant. Interestingly, LAR and SLA were generally higher in the

BW, SW, and HS treatments compared to the FW treatments. Previous studies have found inconsistent effects of salinity on mangrove LAR and SLA. Some studies have found that LAR and SLA are lowest in FW and increase at intermediate salinities, before declining at higher salinities (e.g. Ball 2002, Nguyen et al. 2015). Other studies have found that SLA steadily declines with increasing salinity (Bompy et al. 2014, Nguyen et al. 2017). Yet others have found that LAR and SLA can remain steady or even increase with increasing salinity (e.g. Ball and Pidsley 1995). We conclude that salinity effects on biomass allocation and leaf area traits are likely complex and vary among species and heterogeneity in salinity.

In seedlings of *A. germinans*, we found that salinity had little effect on photosynthetic and respiratory capacity and did not impact photosynthetic and respiratory responses to temperature and *D* across seasons. These results provide new insight into the physiological response of mangroves to seasonal changes in atmospheric conditions, which could advance predictions of $CO_2$ fluxes from mangrove ecosystems in response to changing climate. Future studies that explore factors contributing to temporal and spatial variability in mangrove leaf physiology and thermal acclimation of mangrove photosynthesis, especially in response to climate warming, will further advance our understanding of photosynthetic and respiratory C fluxes in mangroves.

**Acknowledgements**

This research was supported by a grant awarded to MJA from the University of North Florida Environmental Center. Additional support for MF was provided by a grant from the National Science Foundation Research Experience for Undergraduates Program (OCE - 1852488). The authors have no conflicts of interest to declare.

**Author contributions**

MJA led the experimental design, collected leaf gas-exchange data, coordinated the experimental implementation, and led the data analysis and writing. MF, KH, MO, VJ, AN, and MC assisted with experimental implementation and data collection. JC assisted with data analysis and interpretation. ICF provided the seedlings for the experiment and assisted with data interpretation. All authors assisted with editing and writing.

**Data and materials availability**

All methods and data will be made available upon publication of this manuscript.

## References

Akaji Y, Inoue T, Tomimatsu H, Kawanishi A (2019) Photosynthesis, respiration, and growth patterns of *Rhizophora stylosa* seedlings in relation to growth temperature. Trees 33:1041-1049.

Alongi DM (2014) Carbon cycling and storage in mangrove forests. Ann Rev Marine Sci 29:331-349.

Andrews TJ, Muller GJ (1985) Photosynthetic gas exchange of the mangrove, *Rhizophora stylosa* Griff., in its natural environment. Oecologia 65:49-455.

Aspinwall MJ, Drake JE, Campany C, Vårhammar A, Ghannoum O, Tissue DT, Reich PB, Tjoelker MG (2016) Convergent acclimation of leaf photosynthesis and respiration to prevailing ambient temperatures under current and warmer climates in *Eucalyptus tereticornis*. New Phytol 212:354–367.

Aspinwall MJ, Varhammar A, Blackman CJ, Tjoelker MG, Ahrens C, Byrne M, Tissue DT, Rymer PD. (2017). Adaptation and acclimation both influence photosynthetic and respiratory temperature responses in *Corymbia calophylla*. Tree Physiol 37:1095-1112.

Atwood TB, Connolly RM, Almahasheer H, Carnell PE, Duarte CM, Ewers Lewis CJ, Irigoien X, Kelleway JJ, Lavery PS, Macreadie PI, Serrano O, Sanders CJ, Santos I, Steven ADL, Lovelock CE (2017) Global patterns in mangrove soil carbon stocks and losses. Nature Climate Change 7:523–528

Atkin OK, Tjoelker MG (2003) Thermal acclimation and the dynamic response of plant respiration to temperature. Trends Plant Sci 8:343-351.

Atkin OK, Bloomfield KJ, Reich PB et al. (2015) Global variability in leaf respiration in relation to climate, plant functional types and leaf traits. New Phytol 206:614–636.

Ball MC, Farquhar GD (1984) Photosynthetic and stomatal responses of two mangrove species, *Aegiceras corniculatum* and *Avicennia mariana*, to long term salinity and humidity conditions. Plant Physiol 74:1-6.

Ball MC (1988) Ecophysiology of mangroves. Trees 2:129-142.

Ball MC, Cowan IR, Farquhar GD (1988) Maintenance of leaf temperature and the optimization of carbon gain in relation to water loss in a tropical mangrove forest. Aus J Plant Physiol 15:263-276.

Ball MC, Pidsley SM (1995) Growth responses to salinity in relation to distribution of two mangrove species, *Sonneratia alba* and *S. lanceolata*, in northern Australia. Functional Ecol 9:77-85.

Ball MC (2002) Interactive effects of salinity and irradiance on growth: implications

for mangrove forest structure along salinity gradients. Trees 16:126-139.

Battaglia M, Beadle C, Loughhead S (1996) Photosynthetic temperature responses of *Eucalyptus globulus* and *Eucalyptus nitens*. Tree Physiol 16:81–89.

Bauer JE, Cai W-J, Raymond PA, Bianchi TS, Hopkinson CS, Regnier PAG (2013) The changing carbon cycle of the coastal ocean. Nature 504:61-70.

Bompy F, Lequeue G, Imbert D, Dulormne M (2014) Increasing fluctuations of soil salinity affect seedling growth performances and physiology in three Neotropical mangrove species. Plant Soil 380:399-413.

Bouillon S, Borges AV, Castañeda-Moya E, Diele K. (2008) Mangrove production and carbon sinks: A revision of global budget estimates. Global Biogeo Cycles 22, doi:10.1029/2007GB003052

Burchett MD, Clarke CJ, Field CD, Pulkownik A (1989) Growth and respiration in two mangrove species at a range of salinities. Physiol Plantarum 75:299-303.

Canadell JG, Le Quere C, Raupach MR, Field CB, Buitenhuis ET, Ciais P, Conway TJ, Gillett NP, Houghton RA, Marland G (2007) Contributions to accelerating atmospheric CO2 growth from economic activity, carbon intensity, and efficiency of natural sinks. PNAS 104:18866–18870.

Cavanaugh KC, Kellner JR, Forde AJ, Gruner DS, Parker JD, Rodriguez W, Feller IC (2014) Poleward expansion of mangroves is a threshold response to decreased frequency of extreme cold events. PNAS 111:723-727.

Cavanaugh KC, Osland MJ, Bardou, R, Hinojosa-Arango G, López-Vivas JM, Parker JD, Rovai AS (2018) Sensitivity of mangrove range limits to climate variability. Global Ecology and Biogeography 27:925-935

Cheeseman JM, Herendeen LB, Cheeseman AT, Clough BF (1997) Photosynthesis and photoprotection in mangroves under field conditions. Plant Cell Environ 20:579-588.

Clough BF, Sim RG (1982) Changes in gas exchange characteristics and water use efficiency of mangroves in response to salinity and vapour pressure deficit. Oecologia 79:38-44.

Crous KY, Quentin AG, Lin Y-S, Medlyn BE, Williams DG, Barton CVM, Ellsworth DS (2013) Photosynthesis of temperate *Eucalyptus globulus* trees outside their native range has limited adjustment to elevated $CO_2$ and climate warming. Global Change Biol 19:3790–3807,

Cunningham SC (2004) Stomatal sensitivity to vapour pressure deficit of temperate and tropical evergreen rainforest trees of Australia. Trees 18:399-407.

Donato DC, Kauffman JB, Murdiyarso D, Kurnianto S, Stidham M, Kanninen M (2011) Mangroves among the most carbon-rich forests in the tropics. Nature Geoscience 4:293–297

Drake JE, Aspinwall MJ, Pfautsch S, Rymer PD, Reich PB, Smith RA, Crous KY, Tissue DT, Ghannoum O, Tjoelker MG (2015) The capacity to cope with climate warming declines from temperate to tropical latitudes in two widely distributed *Eucalyptus* species. Glob Change Biol 21:459-472.

Dreyer E, Le Roux X, Montpied P, Daudet FA, Masson F (2001) Temperature response of leaf photosynthetic capacity in seedlings from seven temperate tree species. Tree Physiol 21:223-232.

Duarte CM, Losada IJ, Hendriks IE, Mazarrasa I, Marba N (2013) The role of coastal plant communities for climate change mitigation and adaptation. Nature Climate Change 3:961-968.

Duarte CM (2017) Reviews and syntheses: Hidden forests, the role of vegetated coastal habitats in the ocean carbon budget. Biogeosciences 14:301-310.

Duke NC, Ball MC, Ellison JC (1998) Factors influencing biodiversity and distributional gradients in mangroves. Global Ecol Bio Lett 7:27-47.

Ewe SML, Sternberg L, Childers DL (2007) Seasonal plant water uptake patterns in the saline southeast Everglades ecotone. Oecologia. 152:607-616.

Farquhar GD, von Caemmerer S, Berry JA (1980) A biochemical model of $CO_2$ carbon dioxide assimilation in leaves of $C_3$ carbon pathway species. Planta 149:78-90.

IPCC (2013) Stocker TF, Qin D, Plattner G-K, Tignor M, Allen SK, Boschung J, Nauels A, Xia Y, Bex V, Midgley PM, eds. Climate Change 2013: The Physical Science Basis. Contribution of Working Group I to the Fifth Assessment Report of the Intergovernmental Panel on Climate Change. Cambridge, UK & New York, NY, USA: Cambridge University Press.

Jahnke S, Krewitt M (2002) Atmospheric $CO_2$ concentration may directly affect leaf respiration measurement in tobacco, but not respiration itself. Plant Cell Environ 25:641-651.

Kattge J, Knorr W (2007) Temperature acclimation in a biochemical model of photosynthesis: a reanalysis of data from 36 species. Plant Cell Environ 30:1176-1190.

Komiyama A, Eong Ong J, Poungparn S (2008) Allometry, biomass, and productivity of mangrove forests: a review. Aquatic Botany 89:128-137.

Körner C, Cochrane PM (1985) Stomatal responses and water relations of *Eucalyptus pauciflora* in summer along an elevation gradient. Oecologia 66:443-455.

Kosugi Y, Matsuo N (2006) Seasonal fluctuations and temperature dependences of leaf gas exchange parameters of co-occurring evergreen and deciduous trees in a temperature broad-leaved forest. Tree Physiol 26:1173-1184.

Krauss KW, Twilley RR, Doyle TW, Gardiner ES (2006) Leaf gas exchange characteristics of three neotropical mangrove species in response to varying hydroperiod. Tree Physiol 26:959-968.

Krauss KW, Lovelock CE, McKee KL, López-Hoffman L, Ewe SML, Sousa WP (2008) Environmental drivers in mangrove establishment and early development: a review. Aquatic Botany 89:105-127.

Kumarathunge DP, Medlyn BE, Drake JE, Tjoelker MG, Aspinwall MJ, Battaglia M, Cano FJ, Carter KR, Cavaleri MA, Cernusak LA, Chambers JQ, Crous KY, De Kauwe MG, Dillaway DN, Dreyer E, Ellsworth DS, Ghannoum O, Han Q, Hikosaka K, Jensen AM, Kelly JWG, Kruger EL, Mercado LM, Onoda Y, Reich PB, Rogers A, Slot M, Smith NG, Tarvainen L, Tissue DT, Togashi HF, Tribuzy ES, Uddling J, Vårhammar A, Wallin G, Warren JM, Way DA (2019) Acclimation and adaptation components of the temperature dependence of plant photosynthesis at the global scale. New Phytol 222: 768–784.

Lambs L, Muller E, Fromard F (2008) Mangrove trees growing in a very saline condition but not using seawater. Rapid Comm Mass Spec 22:2835-2943.

Lawrence D, Fisher R, Koven C, Oleson K, Swenson S, Vertenstein M, Andre B, Bonan G, Ghimire B, van Kampenhout L, Kennedy D, Kluzek E, Knox R, Lawrence P, Li F, Li H, Lombardozzi D, Lu Y, Perket J, Riley W, Sacks W, Shi M, Wieder W, Xu C, Ali A, Badger A, Bisht G, Broxton P, Brunke M, Buzan J, Clark M, Craig T, Dahlin K, Drewniak B, Emmons L, Fisher J, Flanner M, Gentine P, Lenaerts J, Levis S, Leung LR, Lipscomb W, Pelletier J, Ricciuto DM, Sanderson B, Shuman J, Slater A, Subin Z, Tang J, Tawfik A, Thomas Q, Tilmes S, Vitt F, Zeng X (2018) Technical description of version 5.0 of the Community Land Model (CLM).

Lee TD, Reich PB, Bolstad PV (2005) Acclimation of leaf respiration to temperature is rapid and related to specific leaf area, soluble sugars and leaf nitrogen across three temperate deciduous tree species. Funct Ecol 19:640–647.

Lin G, Sternberg LD (1993) Effects of salinity fluctuation on photosynthetic gas exchange and plant growth of the red mangrove (*Rhizophora mangle* L.). J Exp Bot 44:9–16.

Lombardozzi DL, Bonan GB, Smith NG, Dukes JS, Fisher RA (2015) Temperature acclimation of photosynthesis and respiration: a key uncertainty in the carbon cycle-climate feedback. Geophysical Res Letters 42:8624-8631.

López-Hoffman L, Anten NPR, Martínez-Ramos M, Ackerly DD (2007) Salinity and light interactively affect neotropical mangrove seedlings at the leaf and whole plant levels. Oecologia 150:545-556.

Lovelock CE, Feller IC (2003) Photosynthetic performance and resource utilization of two mangrove species coexisting in a hypersaline scrub forest. Oecologia 134:455-462.

Mcleod E, Chmura GL, Bouillon S, Salm R, Björk M, Duarte CM, Lovelock CE, Schlesinger WH, Silliman BR (2011) A blueprint for blue carbon: toward an improved understanding of the role of vegetated coastal habitats in sequestering $CO_2$. Frontiers Ecol Environ 9:552–560.

Medlyn BE, Dreyer E, Ellsworth D, Forstreuter M, Harley PC, Kirschbaum MUF, Le Roux X, Montpied P, Strassemeyer J, Walcroft A, Wang K, Loustau D (2002) Temperature response of parameters of a biochemically based model of photosynthesis. II. A review of experimental data. Plant Cell Environ 25:1167–1179.

Munns R, Tester M (2008) Mechanisms of salinity tolerance. Ann Rev Plant Bio 59:651-681.
Novick KA, Ficklin DL Stoy PC Williams CA, Bohrer G, Oishi AC, Papuga SA, Blanken PD, Noormets A, Sulman BN, Scott RL, Wang L, Phillips RP (2016) The increasing importance of atmospheric demand for ecosystem water and carbon fluxes. Nature Climate Change 6:1023–1027

Nguyen HT, Stanton DE, Schmitz N, Farquhar GD, Ball MC (2015) Growth responses of the mangrove *Avicennia marina* to salinity: development and function of shoot hydraulic systems require saline conditions. Ann Bot 113:397-407

Nguyen HT, Meir P, Sack L, Evans JR, Oliveira RS, Ball MC (2017) Leaf water storage increases with salinity and aridity in the mangrove *Avicennia marina*: integration of leaf structure, osmotic adjustment and access to multiple water sources. Plant Cell Environ 40:1576-1591.

Oren R, Sperry JS, Katul GG, Pataki DE, Ewers BE, Phillips N, Schäfer KVR (1999) Survey and synthesis of intra- and interspecific variation in stomatal sensitivity to vapour pressure deficit. Plant Cell Environ 22:1515-1526.

Osland MJ, Enwright N, Day RH, Doyle TW (2013) Winter climate change and coastal wetland foundation species: salt marshes vs. mangrove forests in the southeastern United States. Global Change Biology 19:1482-1494.

O'Sullivan OS, Heskel MA, Reich PB, Tjoelker MG, Weerasinghe LK, Penillard A, Zhu L, Egerton JJG, Bloomfield KJ, Creek D, Bahar NHA, Griffin KL, Hurry V, Meir P, Turnbull MH, Atkin OK (2017) Thermal limits of leaf metabolism across biomes. Global Change Biol 23:209-223.

Parida AK, Jha (2010) Salt tolerance mechanisms in mangroves: a review. Trees 24:199-217.

Pezeshki SR, DeLaune RD, Patrick WH (1990) Differential response of selected mangroves to soil flooding and salinity: gas exchange and biomass partitioning. Can J For Res 20:869-874.

Popp M (1995) Salt resistance in herbaceous halophytes and mangroves. Prog Bot 56:416–429.

Prentice IC, Farquhar GD, Fasham MJR, Goulden ML, Heimann M, Jaramillo VJ, Kheshi HS, Le Quere C, Scholes RJ, Wallace DWR. 2001. The carbon cycle and atmospheric carbon dioxide. In: Houghton JT, Ding Y, Griggs DJ, Noguer M, van der Linden PJ, Dai X, Maskell K, Johnson CA, eds. Climate Change 2001: the scientific basis. Contribution of Working Group I to the third assessment report of the Intergovernmental Panel on Climate Change. Cambridge, UK: Cambridge University Press, 183–237.

Reef R, Winter K, Morales J, Adame MF, Reef DL, Lovelock CE (2015a) The effect of atmospheric carbon dioxide concentrations on the performance of the mangrove *Avicennia germinans* over a range of salinities. Physiol Plantarum 154:358–368.

Reef R, Markham HL, Santini NS, Lovelock CE (2015b) The response of the mangrove *Avicennia marina* to heterogeneous salinity measured using a split-root approach. Plant Soil 393:297-305.

Reef R, Lovelock CE (2015) Regulation of water balance in mangroves. Ann Bot 115:385–395.

Reef R, Slot M, Motro U, Motro M, Motro Y, Adame MF, Garcia M, Aranda J, Lovelock CE, Winter K (2016) The effects of CO2 and nutrient fertilization on the growth and temperature response of the mangrove *Avicennia germinans*. Photosynth Res 129:159-170.

Robakowski P, Montpied P, Dreyer E (2002) Temperature response of photosynthesis of silver fir (*Abies alba* Mill.) seedlings. Ann For Sci 59:163-170.

Rodríguez-Calcerrada J, Atkin OK, Robson TM, Zaragoza-Castells J, Gil L, Aranda I (2005) Thermal acclimation of leaf dark respiration of beech seedlings experiencing summer drought in high and low light environments. Tree Phsyiol 30: 214–224

Saintilan N, Wilson NC, Rogers K, Rajkaran A, Krauss KW (2014) Mangrove expansion and salt marsh decline at mangrove poleward limits. Global Change Biol 20:147-157.

Slot M, Kitajima K (2015) General patterns of acclimation of leaf respiration to elevated temperatures across biomes and plant types. Oecologia 177:885-900.

Smith JAC, Popp M, Lüttge U, Cram WJ, Diaz M, Griffiths H, Lee HSJ, Medina E, Schäfer C, Stimmel K-H, Thonke B (1989) Ecophysiology of xerophytic and halophytic vegetation of a coastal alluvial plain in northern Venezuela. VI. Water relations and gas exchange in mangroves. New Phytol 111:293-307.

Smith NG, Malyshev SL, Shevliakova E, Kattge J, Dukes JS (2016) Foliar temperature acclimation reduces simulated carbon sensitivity to climate. Nature Climate Change 6:407-411.

Smith NG, Lombardozzi D, Tawfik A, Bonan G, Dukes JS (2017) Biophysical consequences of photosynthetic temperature acclimation for climate. Journal of Advances in Modeling Earth Systems 9:536–547, doi:10.1002/ 2016MS000732

Smith NG, Dukes JS (2017) Short-term acclimation to warmer temperatures accelerates leaf carbon exchange processes across plant types. Global Change Biol 23: 4840-4853.

Sobrado MA (1999) Leaf photosynthesis of the mangrove *Avicennia germinans* as affected by NaCl. Photosynthetica 36:547-555.

Sobrado MA, Ewe SML (2006) Ecophysiological characteristics of *Avicennia germinans* and *Laguncularia racemosa* coexisting in a scrub mangrove forest at the Indian River Lagoon, Florida. Trees 20:679–687

Suárez, N, Sobrado MA, Medina E (1998) Salinity effects on the leaf water relations components and ion accumulation patterns in *Avicennia germinans*. Oecologia 114:299-304.

Suárez N, Medina E (2005) Salinity effect on plant growth and leaf demography of the mangrove, *Avicennia germinans* L. Trees 19:721–727.

Suárez N, Medina E (2006) Influence of salinity on Na+ and K+ accumulation, and gas exchange in *Avicennia germinans*. Photosynthetica 44:268-274.

Tjoelker MG, Oleksyn J, Reich PB, ˙ Zytkowiak R (2008) Coupling of respiration, nitrogen, and sugars underlies convergent temperature acclimation in *Pinus banksiana* across wide-ranging sites and populations. Glob Chang Biol 14:782–797.

Tjoelker MG, Oleksyn J, Lorenc-Plucinska G, Reich PB (2009) Acclimation of respiratory temperature responses in northern and southern populations of *Pinus banksiana*. New Phytol 181:218–229.

Way DA, Yamori W (2014) Thermal acclimation of photosynthesis: on the importance of adjusting our definitions and accounting for thermal acclimation of respiration. Photosynth Res 119:89-100.

West G, Inzé D, Beemster GTS (2004) Cell cycle modulation in the response of the primary root of *Arabidopsis* to salt stress. Plant Physiol 135:1050–1058

Xu L, Baldocchi DD (2003) Seasonal trends in photosynthetic parameters and stomatal conductance of blue oak (*Quercus douglasii*) under prolonged summer drought and high temperature. Tree Physiol 23:865-877.

**Figure captions**

**Figure 1.** Mean values (± standard error, *n*=9) of stem volume in black mangrove (*Avicennia germinans*) seedlings over time and in response to salinity treatments (FW = freshwater (0 ppt), BW = brackish water (18 ppt), SW = seawater (35 ppt), HS = hypersaline (55 ppt).

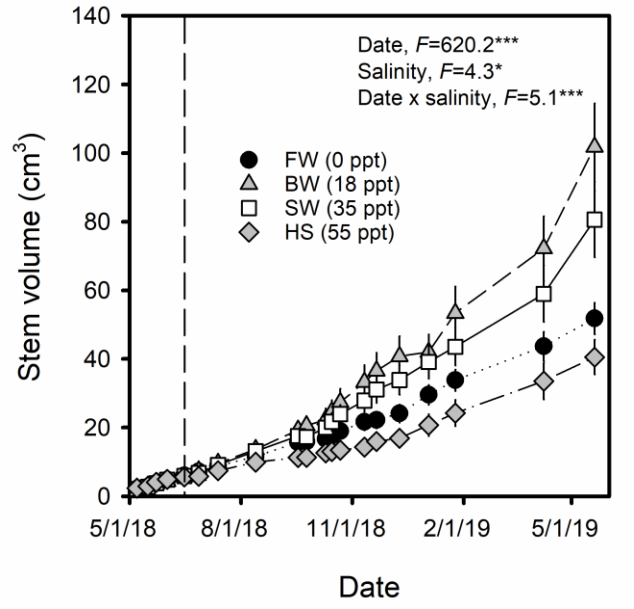

**Figure 2.** (a,b,c) Mean values (± standard error, *n*=3-6) of leaf-level light-saturated net photosynthesis ($A_{sat}$), stomatal conductance to water vapor ($g_s$), and the ratio intercellular $CO_2$ ($C_i$) to atmospheric $CO_2$ ($C_a$) of black mangrove (*Avicennia germinans*) over time and under different salinity treatments (FW = freshwater (0 ppt), BW = brackish water (18 ppt), SW = seawater (35 ppt), HS = hypersaline (55 ppt). (d,e,f) The response of $A_{sat}$, $g_s$, and $C_i/C_a$ to seasonal changes in prevailing leaf temperature ($T_{leaf}$). (g,h,i) The response of $A_{sat}$, $g_s$, and $C_i/C_a$ to changes in prevailing vapor pressure deficit ($D$) at the leaf surface. Note, in panels g and h, $A_{sat}$ and $g_s$ data collected at low $T_{leaf}$ and $D$ did not fit the trajectory of data collected at higher $T_{leaf}$ and $D$. For simplicity, data obtained at $T_{leaf}$ < 20 °C (circled) were not included in model fits. Parameter estimates describing the fitted lines in panels d and e are show in Table 3.

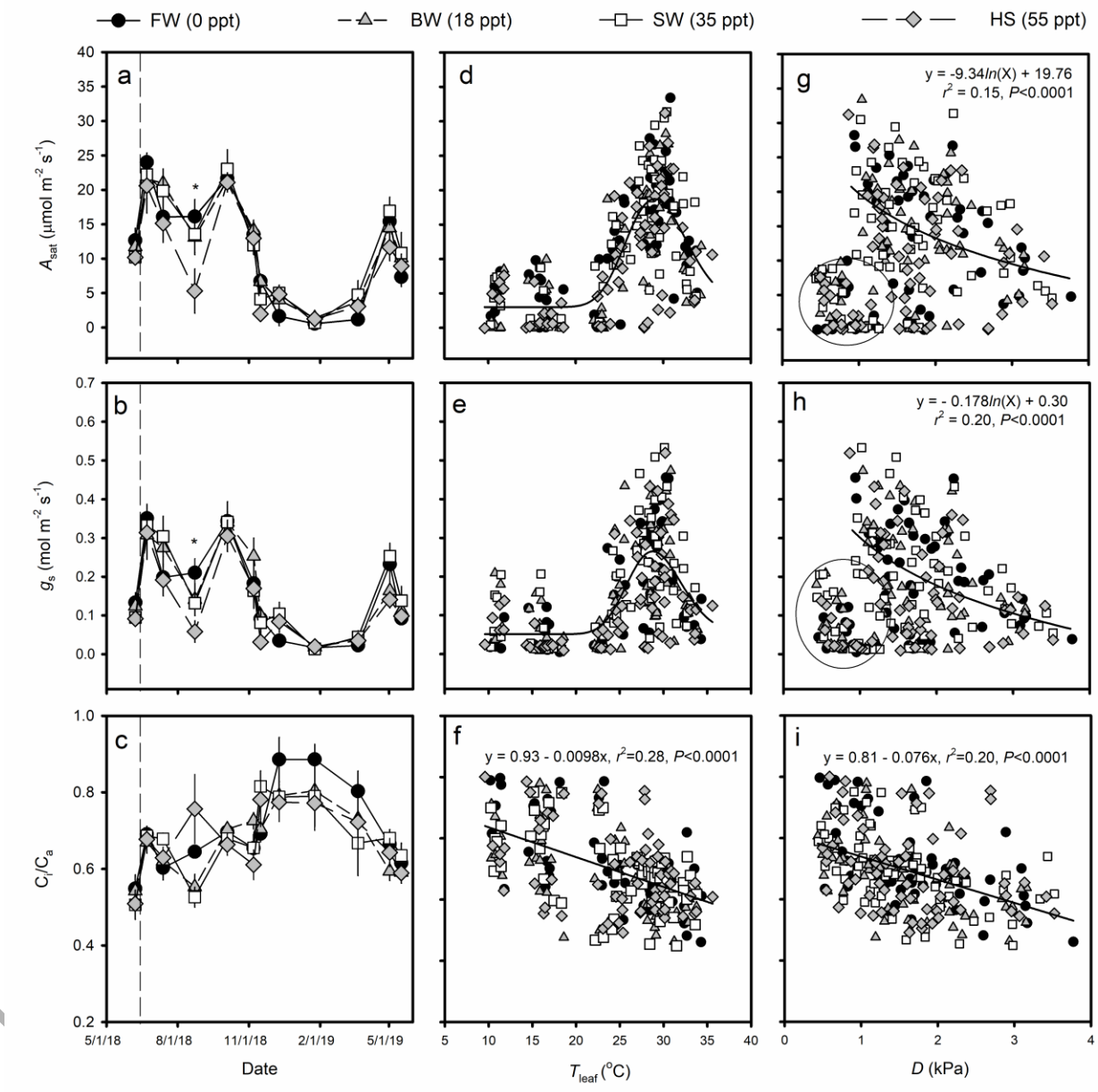

**Figure 3.** (a,b,c) Mean values (± standard error, $n$=3-6) of the maximum rate of Rubisco carboxylation ($V_{cmax}$), the maximum rate of electron transport for RuBP regeneration ($J_{max}$), and the ratio of $J_{max}$ to $V_{cmax}$ of black mangrove (*Avicennia germinans*) over time and under different salinity treatments (FW = freshwater (0 ppt), BW = brackish water (18 ppt), SW = seawater (35 ppt), HS = hypersaline (55 ppt). (d,e,f) The response of $V_{cmax}$, $J_{max}$, and $J_{max}/V_{cmax}$ to seasonal changes in prevailing leaf temperature ($T_{leaf}$). Parameter estimates describing the fitted lines in panels d and e are show in Table 3.

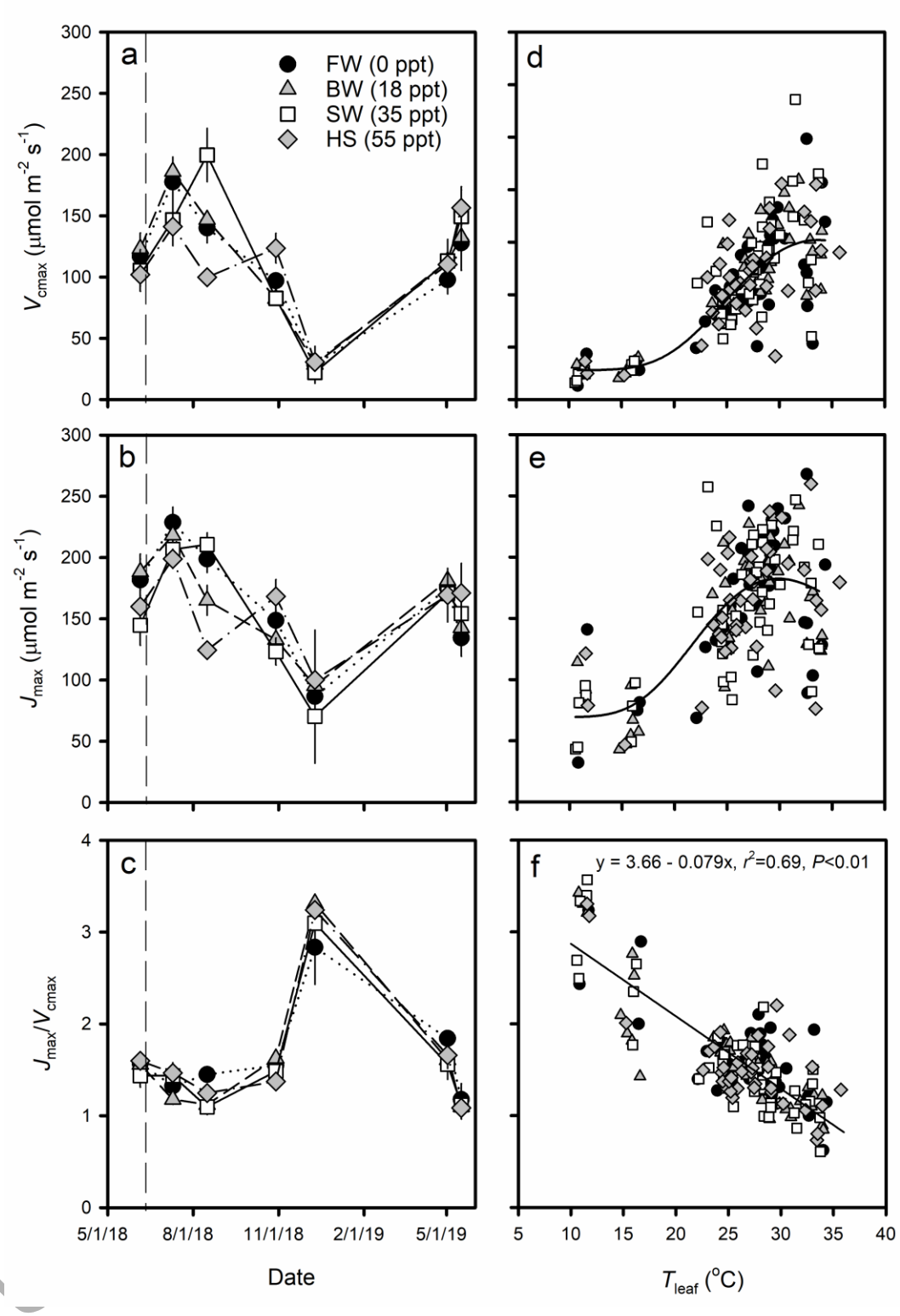

**Figure 4. (a)** Mean values (± standard error, *n*=6) of leaf dark respiration per unit area measured at 25 °C ($R_{area}^{25}$) of black mangrove (*Avicennia germinans*) over time and under different salinity treatments (FW = freshwater (0 ppt), BW = brackish water (18 ppt), SW = seawater (35 ppt), HS = hypersaline (55 ppt). (b) The relationship between $R_{area}^{25}$ and the mean daily air temperature of the previous 5 days.

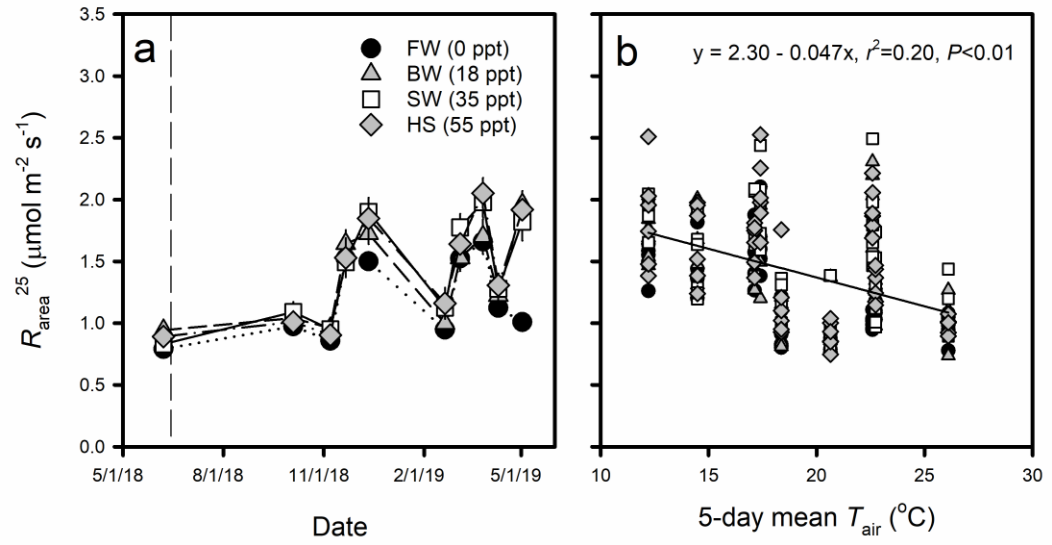

**Table 1.** One-way analysis of variance of salinity effects (degrees of freedom = 3) on component (e.g. root, stem) and total seedling dry mass (DM) production, biomass allocation, and leaf area traits in black mangrove (*Avicennia germinans*). Treatment means (± standard error, n = 9) for each variable are provided for each salinity treatment (freshwater (FW), brackish (BW), seawater (SW), hypersaline (HS)). Treatment means with different letters are significantly different at $P < 0.05$.

| | Salinity effect | Treatment means | | | |
|---|---|---|---|---|---|
| Variable | *F*-value | FW (0 ppt) | BW (18 ppt) | SW (35 ppt) | HS (55 ppt) |
| Root DM (g) | 4.75* | $36.9 \pm 4.3^{a}$ | $81.3 \pm 13.5^{b}$ | $75.6 \pm 5.8^{b}$ | $49.2 \pm 12.8^{ab}$ |
| Stem DM (g) | 10.65** | $22.0 \pm 1.7^{ab}$ | $41.2 \pm 4.9^{c}$ | $32.4 \pm 3.8b^{c}$ | $17.8 \pm 2.6^{a}$ |
| Branch DM (g) | 7.80** | $21.6 \pm 2.4^{a}$ | $42.4 \pm 7.0^{b}$ | $38.9 \pm 4.6^{b}$ | $18.0 \pm 3.7^{a}$ |
| Leaf DM (g) | 8.98** | $29.7 \pm 2.5^{a}$ | $62.2 \pm 9.1^{b}$ | $57.0 \pm 6.0^{b}$ | $31.2 \pm 5.6^{a}$ |
| Total DM (g) | 7.92** | $110.2 \pm 9.1^{a}$ | $227.1 \pm 33.0^{b}$ | $203.9 \pm 16.9^{b}$ | $116.2 \pm 23.4^{a}$ |
| RMF ($g\ g^{-1}$) | 1.55 | $0.33 \pm 0.02^{a}$ | $0.35 \pm 0.02^{a}$ | $0.38 \pm 0.02^{a}$ | $0.39 \pm 0.03^{a}$ |
| SMF ($g\ g^{-1}$) | 2.40 | $0.40 \pm 0.02^{a}$ | $0.38 \pm 0.02^{a}$ | $0.34 \pm 0.02^{a}$ | $0.33 \pm 0.02^{a}$ |
| LMF ($g\ g^{-1}$) | 0.21 | $0.27 \pm 0.01^{a}$ | $0.28 \pm 0.01^{a}$ | $0.28 \pm 0.01^{a}$ | $0.28 \pm 0.01^{a}$ |
| LA ($m^2$) | 12.75*** | $0.16 \pm 0.01^{a}$ | $0.40 \pm 0.05^{b}$ | $0.39 \pm 0.04^{b}$ | $0.21 \pm 0.03^{a}$ |
| LAR ($cm^2\ g^{-1}$) | 6.52** | $14.8 \pm 0.4^{a}$ | $17.9 \pm 0.9^{ab}$ | $19.3 \pm 0.8^{b}$ | $19.8 \pm 1.3^{b}$ |
| SLA ($cm^2\ g^{-1}$) | 11.39*** | $54.9 \pm 1.4^{a}$ | $64.8 \pm 2.5^{b}$ | $70.0 \pm 2.3^{b}$ | $71.1 \pm 2.9^{b}$ |

Note: *F*-values denoted with "***", "**", and "*", are significant at $P < 0.001$, $P < 0.01$, and $P < 0.05$, respectively.

Variable descriptions: RMF, root mass fraction (Root DM/Total DM); SMF, stem mass fraction (Stem DM + Branch DM) / Total DM); LMF, leaf mass fraction (Leaf DM/Total DM); LA, whole-tree leaf area; LAR, leaf area ratio (LA/Total DM); SLA, specific leaf area (whole-tree LA/Leaf DM).

**Table 2.** Analysis of variance of measurement date, salinity treatment, and date × salinity effects on leaf-level physiological traits in black mangrove (*Avicennia germinans*). Numerator and denominator degree of freedom (*df*) and *F*-values are presented for each trait and fixed effect. Mean (± standard error) values for each leaf trait are provided for each salinity treatment (freshwater (FW), brackish (BW), seawater (SW), hypersaline (HS)).

| | Date | | Salinity | | Date × Salinity | | Treatment means | | | |
|---|---|---|---|---|---|---|---|---|---|---|
| Variable | *df* | *F* | *df* | *F* | *df* | *F* | FW (0 ppt) | BW (18 ppt) | SW (35 ppt) | HS (55 ppt) |
| $A_{sat}$ (μmol $m^{-2}$ $s^{-1}$) | 10,184 | 61.1*** | 3,28 | 3.6* | 30,184 | 1.6* | 11.3 ± 1.1 | 12.1 ± 1.0 | 11.9 ± 1.1 | 9.78 ± 1.0 |
| $g_s$ (mol $m^{-2}$ $s^{-1}$) | 10,187 | 57.1*** | 3,28 | 4.0* | 30,187 | 1.6* | 0.162 ± 0.02 | 0.170 ± 0.02 | 0.171 ± 0.02 | 0.133 ± 0.02 |
| $C_i/C_a$ | 10,187 | 10.9*** | 3,28 | 1.0 | 30,187 | 1.3 | 0.714 ± 0.02 | 0.679 ± 0.02 | 0.691 ± 0.02 | 0.692 ± 0.02 |
| $V_{cmax}$ (μmol $m^{-2}$ $s^{-1}$) | 5,75 | 71.4*** | 3,28 | 0.2 | 15,75 | 1.9* | 120.0 ± 9.0 | 122.8 ± 8.3 | 121.8 ± 11.0 | 123.3 ± 8.8 |
| $J_{max}$ (μmol $m^{-2}$ $s^{-1}$) | 5,75 | 26.0*** | 3,28 | 0.3 | 15,75 | 2.0* | 169.8 ± 9.0 | 161.5 ± 7.2 | 158.5 ± 9.3 | 167.7 ± 8.9 |
| $J_{max}/V_{cmax}$ | 5,75 | 100.6*** | 3,28 | 0.3 | 15,75 | 1.4 | 1.56 ± 0.09 | 1.51 ± 0.11 | 1.59 ± 0.12 | 1.52 ± 0.11 |
| $R_{area}^{25}$ (μmol $m^{-2}$ $s^{-1}$) | 8,158 | 88.0*** | 3,20 | 5.0** | 24,158 | 3.3*** | 1.24 ± 0.05 | 1.42 ± 0.06 | 1.49 ± 0.06 | 1.50 ± 0.06 |

Note: *F*-values denoted with "***", "**", and "*", are significant at $P < 0.001$, $P < 0.01$, and $P < 0.05$, respectively.

Variable descriptions: $A_{sat}$, light-saturated net photosynthetic rate; $g_s$, stomatal conductance to water vapor; $C_i/C_a$, ratio or intercellular $CO_2$ to atmospheric $CO_2$; $V_{cmax}$, maximum rate of Rubisco carboxylation; $J_{max}$, maximum rate of electron transport for RuBP regeneration; $J_{max}/V_{cmax}$, ratio of $V_{cmax}$ to $J_{max}$; $R_{area}^{25}$, rate of leaf dark respiration per unit area measured at 25 °C. $A_{sat}$ data were square-root transformed and $g_s$, $V_{cmax}$, and $R_{area}^{25}$ data were log-transformed to fulfil assumptions of normality.

**Table 3.** Parameter estimates (± standard error) for an empirical model (Equation 1) describing the long-term temperature response of leaf-level light saturated net photosynthesis ($A_{sat}$), stomatal conductance to water vapor ($g_s$), the maximum rate of Rubisco carboxylation ($V_{cmax}$), and the maximum rate of electron transport for RuBP regeneration ($J_{max}$) in black mangrove (*Avicennia germinans*) seedlings grown under contrasting salinity treatment (freshwater (FW), brackish (BW), seawater (SW), hypersaline (HS)). Parameters *a* and *b* describe the shape of the temperature response. Parameter $y_0$ is the intercept and parameter $x_0$ is an estimate of the $T_{leaf}$ at which each variable is maximal (i.e. the temperature optimum). Models were fit to data from each salinity treatment individually and to data from all treatments combined. If 95% confidence intervals (standard error × 1.96) for parameter estimates overlapped between salinity treatments, then salinity effects were not significant. Parameter estimates that differed significantly between salinity treatments (95% confidence intervals did not overlap) are denoted with different letters. For each model and salinity treatment, the number of observations (*n*) is provided. The coefficient of determination ($r^2$) provides a measure of model fit and the model *F*-value and *P*-value indicate model significance.

| | | Parameters | | | | Model fit | | |
|---|---|---|---|---|---|---|---|---|
| Model: $A_{sat}$ vs $T_{leaf}$ | *n* | *a* | *b* | $x_0$ | $y_0$ | $r^2$ | *F* | *P-value* |
| FW (0 ppt) | 64 | 499.0 ± 44.0 | 0.108 ± 0.01 | 29.2 ± 0.4 | 2.56 ± 1.17 | 0.69 | 43.8 | <0.0001 |
| BW (18 ppt) | 65 | 439.6 ± 45.9 | 0.121 ± 0.02 | 29.3 ± 0.5 | 3.83 ± 1.23 | 0.60 | 31.1 | <0.0001 |
| SW (35 ppt) | 65 | 498.0 ± 48.7 | 0.118 ± 0.02 | 29.3 ± 0.4 | 3.14 ± 1.26 | 0.63 | 35.0 | <0.0001 |
| HS (55 ppt) | 65 | 400.4 ± 59.8 | 0.139 ± 0.03 | 30.0 ± 0.9 | 2.54 ± 1.52 | 0.43 | 15.3 | <0.0001 |
| All treatments | 259 | 459.2 ± 24.7 | 0.120 ± 0.01 | 29.4 ± 0.3 | 3.00 ± 0.65 | 0.58 | 116.7 | <0.0001 |
| Model: $g_s$ vs $T_{leaf}$ | | | | | | | | |
| FW (0 ppt) | 64 | 7.02 ± 0.47 | -0.098 ± 0.02[a] | 29.2 ± 0.43 | 0.044 ± 0.019 | 0.60 | 30.6 | <0.0001 |
| BW (18 ppt) | 65 | 5.67 ± 0.93 | -0.119 ± 0.03[a] | 28.7 ± 0.70 | 0.063 ± 0.025 | 0.38 | 12.7 | <0.0001 |
| SW (35 ppt) | 65 | 6.84 ± 0.88 | -0.099 ± 0.02[a] | 28.9 ± 0.45 | 0.059 ± 0.023 | 0.50 | 20.0 | <0.0001 |
| HS (55 ppt) | 65 | 5.37 ± 0.95 | 0.116 ± 0.03[b] | 29.8 ± 0.84 | 0.042 ± 0.024 | 0.35 | 10.8 | <0.0001 |
| All treatments | 259 | 6.19 ± 0.43 | -0.108 ± 0.01 | 29.1 ± 0.29 | 0.051 ± 0.011 | 0.45 | 68.2 | <0.0001 |
| Model: $V_{cmax}$ vs $T_{leaf}$ | | | | | | | | |
| FW (0 ppt) | 35 | 4488 ± 1945 | 0.273 ± 0.15 | 37.2 ± 9.03 | 28.9 ± 21.5 | 0.53 | 11.6 | <0.0001 |
| BW (18 ppt) | 40 | 4002 ± 317 | 0.156 ± 0.02 | 31.8 ± 0.66 | 31.1 ± 7.9 | 0.83 | 56.8 | <0.0001 |
| SW (35 ppt) | 41 | 6905 ± 6979 | 0.393 ± 0.29 | 45.3 ± 29.98 | 21.7 ± 20.7 | 0.61 | 19.0 | <0.0001 |
| HS (55 ppt) | 32 | 4732 ± 2668 | 0.363 ± 0.24 | 39.9 ± 16.22 | 25.1 ± 26.9 | 0.49 | 9.1 | <0.001 |
| All treatments | 148 | 4444 ± 597 | 0.269 ± 0.06 | 35.8 ± 3.0 | 27.5 ± 8.0 | 0.60 | 73.5 | <0.0001 |
| Model: $J_{max}$ vs $T_{leaf}$ | | | | | | | | |
| FW (0 ppt) | 35 | 3433 ± 613 | 0.140 ± 0.03 | 29.9 ± 0.67 | 82.1 ± 18.7 | 0.54 | 12.1 | <0.0001 |
| BW (18 ppt) | 40 | 3428 ± 362 | 0.153 ± 0.02 | 30.0 ± 0.58 | 73.1 ± 9.8 | 0.72 | 30.3 | <0.0001 |
| SW (35 ppt) | 41 | 3564 ± 662 | 0.277 ± 0.11 | 31.4 ± 3.12 | 68.5 ± 18.3 | 0.52 | 13.6 | <0.0001 |
| HS (55 ppt) | 32 | 3219 ± 880 | 0.214 ± 0.08 | 31.2 ± 2.13 | 82.4 ± 25.7 | 0.35 | 5.0 | <0.01 |
| All treatments | 148 | 3397 ± 274 | 0.183 ± 0.02 | 30.3 ± 0.5 | 76.1 ± 7.9 | 0.53 | 53.1 | <0.0001 |